

## Characterization of a New Caged Proton Capable of Inducing Large pH Jumps

Andreas Barth\* and John E. T. Corrie<sup>†</sup>

\*Institut für Biophysik, Johann Wolfgang Goethe-Universität, D-60590 Frankfurt am Main, Germany, and <sup>†</sup>National Institute for Medical Research, London NW7 1AA, United Kingdom

**ABSTRACT** A new caged proton, 1-(2-nitrophenyl)ethyl sulfate (caged sulfate), is characterized by infrared spectroscopy and compared with a known caged, proton 2-hydroxyphenyl 1-(2-nitrophenyl)ethyl phosphate (caged HPP). In contrast to caged HPP, caged sulfate can induce large pH jumps and protonate groups that have pK values as low as 2.2. The photolysis mechanism of caged sulfate is analogous to that of *P*<sup>3</sup>-[1-(2-nitrophenyl)ethyl] ATP (caged ATP), and the photolysis efficiency is similar. The utility of this new caged compound for biological studies was demonstrated by its ability to drive the acid-induced conformational change of metmyoglobin. This transition from the native conformation to a partially unfolded form takes place near pH 4 and was monitored by near-UV absorption spectroscopy.

### INTRODUCTION

The pH of a biological system is a crucial determinant of the structures and properties of its components, and studies of pH dependencies have a long tradition in biophysics. Many perturbation studies have used rapid mixing techniques, but these are not always appropriate and time resolution below ~1 ms is difficult to achieve. One alternative approach is to use caged compounds, which can generate an active compound from a biologically inactive precursor by flash photolysis (Adams and Tsien, 1993; Corrie and Trentham, 1993; Kaplan, 1990; Kaplan et al., 1978; Marriott, 1998; McCray and Trentham, 1989). In favorable cases, generation of the active species can be effected much more rapidly than by conventional mixing techniques. Here we describe a new caged proton reagent capable of inducing a large and rapid acidification upon photolysis.

Photorelease from the majority of caged compounds is based on the well-known 2-nitrobenzyl rearrangement (Fig. 1; below, numbers in parentheses refer to the numbered products in this figure). In all cases a proton is liberated by ionization of the primary photochemical product, a nitronic acid (1). The rate constant for proton release from the nitronic acid (1) in unbuffered solution has recently been measured as  $\sim 2 \times 10^7 \text{ s}^{-1}$  at 25°C: in the presence of buffer salts, ionization took place within the time of the laser flash (<25 ns; Schwörer and Wirz, 2001). Thus the nitronic acid (1) is in rapid equilibrium with its conjugate *aci*-nitro anion (2). The pK of the nitronic acid is ~3.5 (Schwörer and Wirz, 2001; Wettermark et al., 1965), so the

ionized species predominates in neutral solution. The lifetime of the anion (2) varies over a range of a few microseconds to hundreds of milliseconds, depending on the nature of the attached OR group (Fig. 1). Recent work indicates that decay of the anion (2) to the bicyclic intermediate (3) (Walker et al., 1988) proceeds via the conjugate acid (1), or its isomer protonated on the other oxygen of the nitronic acid, which is reached through rapid equilibration with the anion (2) (Il'ichev and Wirz, 2000; Schwörer and Wirz, 2001). Upon breakdown of the intermediate (3), the photolysis product RO<sup>-</sup> is released and, to an extent dictated by its pK, will neutralize the proton formed by the initial ionization of the nitronic acid (1). Hence, net proton release for the overall reaction may be total, partial, or zero. If RO<sup>-</sup> is a very weak base, full release of one proton per photolyzed molecule will be observed, but if RO<sup>-</sup> is a strong base, the proton will be fully neutralized. The bicyclic intermediate (3) does not normally accumulate, as the rate-limiting step is considered to be reprotonation of the anion (2) (Il'ichev and Wirz, 2000; Schwörer and Wirz, 2001). Therefore, the overall time course for approach to the post-photolysis pH value is a rapid acidification step, nor-

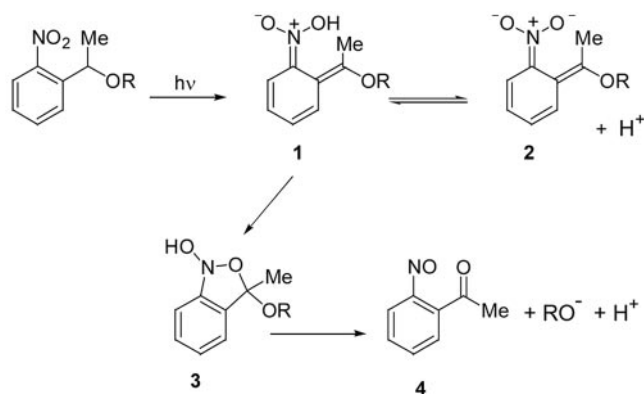


FIGURE 1 Generalized reaction mechanism for photolysis of 1-(2-nitrophenyl)ethyl caged compounds. For caged sulfate, -OR is OSO<sub>3</sub><sup>-</sup>.

Submitted April 22, 2002, and accepted for publication June 12, 2002.

A. Barth's current address: Institute of Biochemistry and Biophysics, The Arrhenius Laboratories for Natural Sciences, Stockholm University, SE-10691 Stockholm, Sweden.

Address reprint requests to Dr. John E. T. Corrie, National Institute for Medical Research, The Ridgeway, Mill Hill, London NW7 1AA, United Kingdom. Tel.: +44-20-8959-3666; Fax: +44-20-8906-4419; E-mail: jcorrie@nimr.mrc.ac.uk.

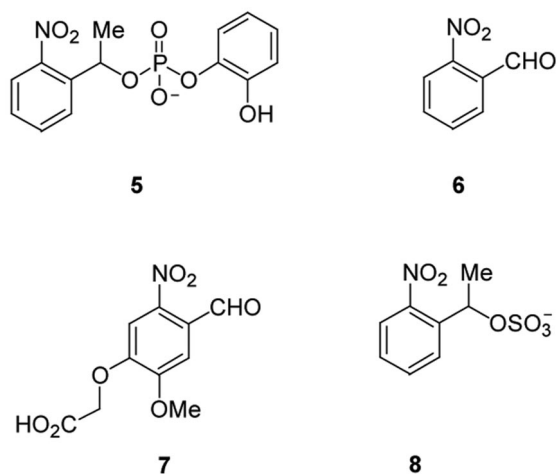


FIGURE 2 Structures of caged proton reagents.

mally within the photolysis pulse, followed by an exponential approach to a new pH value as the *aci*-nitro anion (2) decays to the final products. However, if the pK of the photolysis product  $\text{RO}^-$  is substantially below the pH imposed in the initial jump, no decay of the initial rapid acidification will be observed.

A few compounds that function as caged protons capable of imposing rapid net acidification have been described previously. Among these is 2-hydroxyphenyl 1-(2-nitrophenyl)ethyl phosphate (5) (caged HPP) (Fig. 2). The pK of the released 2-hydroxyphenyl phosphate is 5.3, so caged HPP (5) cannot acidify solutions to values much below pH 5 (Khan et al., 1993). Photochemical rearrangement of 2-nitrobenzaldehydes to 2-nitrosobenzoic acids has also been used as a source of caged protons, either with 2-nitrobenzaldehyde (6) itself (Bonetti et al., 1997; Abbruzzetti et al., 2000) or its water-soluble derivative 4-formyl-6-methoxy-3-nitrophenoxyacetic acid (7) (Janko and Reichert, 1987). The pK of 2-nitrosobenzoic acid does not appear to have been determined but is evidently below 4 (Abbruzzetti et al., 2000). For the water-soluble derivative (7), pK values of the photoproduct were reported as 0.75 and 2.76 (Janko and Reichert, 1987). The former value is a remarkably strong acidity for an aromatic carboxylic acid, but the second pK (for the oxyacetate side chain) would in any case exclude a pH excursion below pH  $\sim 2.5$  for an experiment that began near neutral pH. This discussion excludes the elegant transient acidifications that can be imposed by pulse irradiation of phenolic compounds, for which the first excited state has very much higher acidity than the ground state (Gutman et al., 1981). These transients return to the initial level within a few microseconds, so are not relevant to the enduring acidifications considered here.

One of us (A.B.) has used caged compounds over a number of years to study protein reactions by Fourier transform infrared spectroscopy (FTIR) (Barth, 1999; Barth et

al., 1990, 1996), and this approach is gaining wider adherence (reviewed by Barth and Zscherp, 2000; see also Cheng et al., 2001; Jayaraman et al., 2000). To extend the technique to studies of pH-dependent protein conformational changes and protein folding driven largely by protonation of carboxylate side chains, a caged proton was required that fulfilled three main requirements: 1) the compound should be able to generate a large, permanent pH jump to values below pH 4, 2) proton release should be rapid and proceed with good photolysis efficiency, and 3) the infrared absorbance changes upon photolysis of the reagent should be as few as possible. Although 2-nitrobenzaldehydes (6 and 7) meet the first two criteria, they fail on the third. Photolysis of either compound converts an aldehyde to a carboxylate group, both of which absorb strongly in regions where they would mask absorptions of Asp and Glu side chains and of amide II vibrations that reflect changes in backbone conformation and hydrogen bonding. Thus the caged proton reagents described above do not adequately meet these requirements, and we now describe a new reagent, purpose-designed for infrared spectroscopy, although it may have applications beyond this specific field as it can generate larger pH jumps than other caged protons that have been described.

For this new caged proton, 1-(2-nitrophenyl)ethyl sulfate (8), the released sulfate group has pK 1.92 at 20°C (Perrin, 1982). Hence this caged proton, here called caged sulfate as it also releases a sulfate ion upon photolysis, is capable of generating acidifications down to pH  $\sim 2$ . The released sulfate ion is likely to be inert in the majority of biological systems. We have characterized the properties of caged sulfate and compared them with caged HPP. The applicability of caged sulfate to biological problems is demonstrated by its ability to induce partial unfolding of metmyoglobin (Mb) near pH 4.

## MATERIALS AND METHODS

### Chemicals and biochemicals

Carboxylic acids (Aldrich, Milwaukee, WI) were converted to potassium salts by adjustment of their aqueous solutions or suspensions to pH 7 with 1 M KOH to give 50 mM stock solutions that were further diluted as required for FTIR experiments. Caged HPP was prepared as described (Khan et al., 1993), converted to its sodium salt by exchange with Dowex 50 (Na form), and stored at  $-20^\circ\text{C}$  at  $\sim 100$  mM concentration. Caged ATP, 1-(2-nitrophenyl)ethanol, and 1-(2-nitrophenyl)ethyl phosphate were prepared as described (Walker et al., 1988; Corrie et al., 1992). Triethylamine- $\text{SO}_3$  complex was prepared as described (Tserng and Klein, 1977). Horse heart Mb was from Sigma Chemical Co. (St. Louis, MO).

### Caged sulfate

Caged sulfate was prepared as described for 2-nitrobenzyl sulfate (Corrie et al., 2000). Thus a solution of 1-(2-nitrophenyl)ethanol (167 mg, 1 mmol) in anhydrous dimethyl formamide (Aldrich; 10 ml) was treated with triethylamine- $\text{SO}_3$  complex (200 mg, 1.1 mmol), and the solution was

stirred for 1 h at room temperature and then diluted to 100 ml with water. The solution was adjusted to pH 7 and chromatographed on a column of DEAE-cellulose ( $2 \times 30$  cm) using a linear gradient of triethylammonium bicarbonate (10–200 mM). Fractions were analyzed by anion exchange high-performance liquid chromatography (Whatman SAX column, catalog item 4621–0505) in a mobile phase of 10 mM sodium phosphate, pH 5.5/methanol (10:1 v/v), with a flow rate of  $1.5 \text{ ml min}^{-1}$ . The retention time of the caged sulfate (8) was 2.7 min. Fractions containing the caged sulfate (8) were combined and rotary evaporated under vacuum and then reevaporated from methanol (three times) to remove residual triethylamine. The caged sulfate (8) was obtained in  $\sim 100\%$  yield (based on  $\epsilon_{263}$  of  $4700 \text{ M}^{-1} \text{ cm}^{-1}$  determined for an aqueous solution of 1-(2-nitrophenyl)ethanol) and was converted to its sodium salt (Dowex 50, Na form) for storage in frozen aqueous solution. The compound was characterized by  $^1\text{H}$  NMR spectroscopy that showed  $\delta$  (500 MHz,  $\text{D}_2\text{O}$ , acetone reference) 8.02 (dd,  $J = 8.6$  and  $1.3$  Hz, 1H), 7.83 (dd,  $J = 8.6$  and  $1.3$  Hz, 1H), 7.78 (dt,  $J = 8.6$  and  $1.3$  Hz, 1H), 7.55 (dt,  $J = 8.6$  and  $1.3$  Hz, 1H), 6.01 (q,  $J = 6.5$  Hz, 1H), and 1.68 (d,  $J = 6.5$  Hz, 3H).

The quantum yield for photolysis of caged sulfate was measured by comparison with 1-(2-nitrophenyl)ethyl phosphate. A solution that contained a mixture of the latter compound and caged sulfate (each 0.50 mM) in 20 mM MOPS, pH 7, with 2 mM dithiothreitol (DTT) was irradiated in a Rayonet RPR-100 photochemical reactor equipped with 16 lamps of 350-nm emission maximum (Southern New England Ultraviolet Co., Branford, CT). The extent of conversion of each compound was measured by anion-exchange high-performance liquid chromatography (column as above; mobile phase of 15 mM sodium phosphate, pH 5.5/methanol (20:1 v/v), and flow rate of  $1.5 \text{ mL min}^{-1}$ ). Retention times were 2.4 and 4.8 min for the sulfate and phosphate, respectively, and the corresponding extents of photolysis after 30 s of irradiation for the two compounds were 50.7% and 58.6%. The decay rate of the *aci*-nitro intermediate formed upon flash irradiation of the caged sulfate (8) was determined by time-resolved absorption spectrophotometry at 406 nm as previously described (Walker et al., 1988), except that the photolysis light (347 nm) was from a frequency-doubled ruby laser (Lumonics QSR2/6, Rugby, UK) with a pulse width of  $\sim 30$  ns and average a pulse energy of  $\sim 75$  mJ. The photolysis solutions contained 0.5 mM caged sulfate in 20 mM MOPS, pH 7.0, or 20 mM MES, pH 6.0.

### Sample preparation for FTIR measurements

Samples were prepared by vacuum-drying  $1 \mu\text{l}$  of the relevant carboxylate salt solution and  $1 \mu\text{l}$  of caged proton solution onto a  $\text{CaF}_2$  window with a central circular trough of  $5\text{-}\mu\text{m}$  depth. The sample was rehydrated with  $1 \mu\text{L}$   $^1\text{H}_2\text{O}$  or  $^2\text{H}_2\text{O}$  and closed with a flat  $\text{CaF}_2$  window. Sample concentrations in the infrared (IR) cell were 100 mM caged sulfate or 98 mM caged HPP, with or without one of the following potassium salts: 10 mM acetate, methoxyacetate, 2-nitrobenzoate, or trifluoroacetate. Samples were at pH 7 before photolysis.

### FTIR measurements

FTIR measurements at  $20^\circ\text{C}$  were performed on a modified Bruker IFS66 spectrometer equipped with a HgCdTe detector and running the Bruker Opus program. Data were acquired with double-sided interferograms in a forward-backward mode at a spectral resolution of  $4 \text{ cm}^{-1}$  with the Blackman-Harris four-term apodization function. A reference spectrum was accumulated from 300 interferometer scans, and then photolysis of caged proton reagents was triggered with light from a xenon flash tube that was filtered by a Schott UG11 filter before reaching the sample cell. A sample spectrum was accumulated from 300 interferometer scans, and additional spectra were recorded after one or more additional flashes if desired. Difference spectra calculated from the paired sample and reference spectra show the difference in absorbance for each sample before and after

photolysis. The photolysis efficiency for caged sulfate was 26% in the first flash, as determined from the fractional change in intensity of the negative band at  $1527 \text{ cm}^{-1}$  in the spectra after successive flashes on the same sample.

Time-resolved spectra to determine the spectrum of the *aci*-nitro intermediate of caged sulfate and to study the reaction with DTT of the 2-nitrosoacetophenone by-product from photolysis were acquired under different conditions. For the *aci*-nitro spectrum, the sample contained 128 mM caged sulfate in 400 mM Bicine, pH 8.5, in  $^1\text{H}_2\text{O}$ , and spectra were recorded at  $1^\circ\text{C}$ . Spectra from the time windows 1–320 ms and 16–29 s after the photolysis flash were combined, and results from two successive samples were averaged. For the by-product reactions with DTT, spectra were acquired at  $35^\circ\text{C}$  for a solution in  $^2\text{H}_2\text{O}$  containing 128 mM caged sulfate and 200 mM DTT in 200 mM MES, pH 6 (Barth et al., 1997). Spectra were recorded in the time windows 4–60 ms, 0.32–3.2 s, and 126–185 s after the light flash.

### Metmyoglobin titrations

The titrations with caged sulfate used a UV-visible spectrometer constructed in-house that consisted of a deuterium lamp, quartz fiber optics, and a MCS 55 multichannel spectrometer module (Carl Zeiss, Oberkochen, Germany). A  $20\text{-}\mu\text{l}$  aliquot of sample solution was placed in a microcuvette of 1-mm path length. The cuvette was a modification of the IR cuvette: it had two plane  $\text{CaF}_2$  windows and a 1-mm-thick Teflon spacer with a central 4-mm-diameter hole. The concentrations for the Mb titration samples were as follows: 0.11 mM horse heart Mb, 100 mM NaCl, and 2.5 mM caged sulfate. Control samples contained the same solutes plus 50 mM sodium acetate to buffer the protons released by photolysis of caged sulfate; therefore, no pH change is expected for these samples. The solution of Mb in NaCl and the sodium acetate buffer were each adjusted to pH 4.6 before mixing. Photolysis was triggered by the same xenon flash tube used for the IR experiments.

Titration spectra obtained with the unbuffered Mb titration samples were corrected for the absorbance change of caged sulfate upon photolysis using data from the buffered control samples. The control difference spectra show only the absorbance changes of caged sulfate upon progressive photolysis, and these difference spectra were subtracted from the respective titration spectra, i.e., titration spectrum after the  $n$ th flash minus control difference spectrum after the  $n$ th flash. This procedure largely cancels the absorbance changes of caged sulfate in the titration spectra.

Titrations of horse heart Mb with HCl in a 1-cm-path-length cuvette were performed in a Hitachi U2000 spectrophotometer with 2 ml of a solution of Mb ( $5.5 \mu\text{M}$ ) in 100 mM NaCl.

## RESULTS AND DISCUSSION

### Photolysis chemistry of caged sulfate

Fig. 3 A shows time-resolved IR difference spectra of caged sulfate photolysis, with initial formation of the *aci*-nitro intermediate (*dotted line*) and formation of the final products (*solid line*). Negative bands arise from groups in caged sulfate that are modified in the photolysis reaction, and positive bands are from groups formed upon photolysis in the *aci*-nitro intermediate or the final products. Both the intermediate and final spectra, respectively, are similar to those of other 1-(2-nitrophenyl)ethyl esters such as  $P^3$ -[1-(2-nitrophenyl)ethyl] ATP (caged ATP) (Barth et al., 1995, 1997) and 1-(2-nitrophenyl)ethyl methyl phosphate (caged methyl phosphate) (A. Barth and J. E. T. Corrie, unpublished data). To retard decay of the *aci*-nitro intermediate

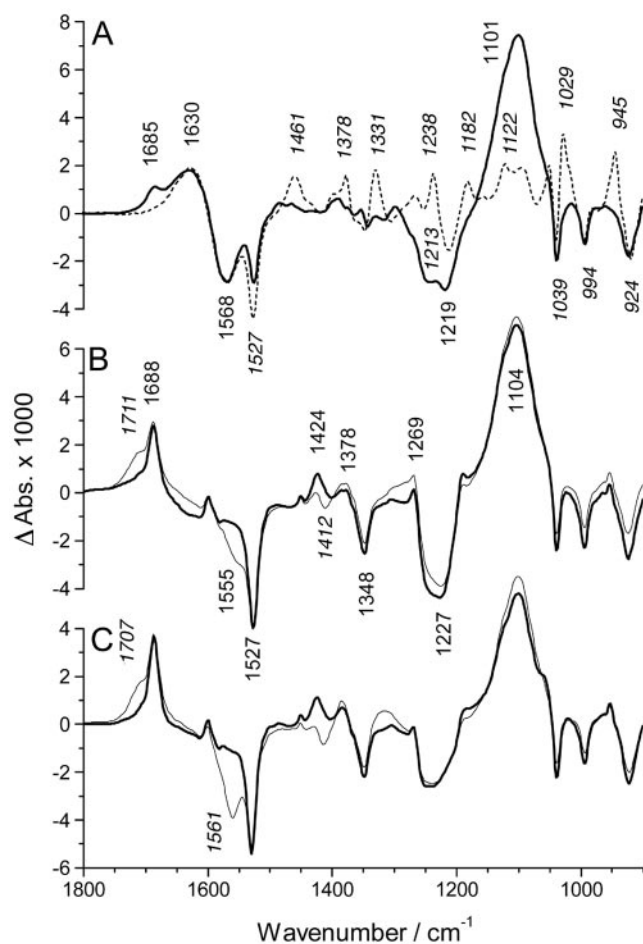


FIGURE 3 IR difference spectra of the photolysis reaction of caged sulfate. (A) Time-resolved spectra of caged sulfate photolysis recorded at 0–0.32 s (*···, italics*) and 16–29 s (*—, normal type*) after the photolysis flash in 400 mM Bicine buffer, pH 8.5, in  $^1\text{H}_2\text{O}$  at  $1^\circ\text{C}$ ; (B and C) Spectra recorded at pH 7.0 and  $20^\circ\text{C}$  in the presence (*thin lines*) or absence of acetate (*bold lines*), which acts as an IR pH indicator. The solvent was  $^1\text{H}_2\text{O}$  (B) or  $^2\text{H}_2\text{O}$  (C) and contained no buffer salts except where acetate was present. The difference between the spectra of samples with and without acetate indicates protonation of acetate caused by the photolysis of caged sulfate. Labels in normal type refer to the spectra recorded without acetate; italic labels refer to the spectra recorded with acetate.

sufficiently to record its spectrum, it was necessary to work at pH 8.5 and  $1^\circ\text{C}$ . A full assignment of the *aci*-nitro spectrum was not part of this work, but its substantial similarity to the corresponding spectrum recorded on photolysis of caged ATP (Barth et al., 1995, 1997) includes bands at 1461, 1378, and  $1331\text{ cm}^{-1}$ . These were previously assigned to vibrations of the nitronate group and are at essentially the same positions as in the caged ATP spectrum (1465, 1379, and  $1330\text{ cm}^{-1}$ ). Both the intermediate and final spectra show strong signals for protonation of the Bicine buffer by the proton released on photolysis (negative band at  $1568\text{ cm}^{-1}$  and positive band at  $1630\text{ cm}^{-1}$ ), as discussed below for other carboxylates.

Fig. 3, B and C, show IR difference spectra of the overall photolysis reaction of caged sulfate in  $^1\text{H}_2\text{O}$  (Fig. 3 B, *bold line*) and  $^2\text{H}_2\text{O}$  (Fig. 3 C, *bold line*) at  $20^\circ\text{C}$  and a starting pH of 7.0 in unbuffered solution. The thin lines (for spectra recorded in the presence of acetate) are discussed below. Negative bands at  $1527$  and  $1348\text{ cm}^{-1}$  are from the anti-symmetric and symmetric stretching vibrations of the nitro group (Barth et al., 1995, 1997), and the band at  $1227\text{ cm}^{-1}$  was assigned to the asymmetric  $\text{SO}_3^-$  stretching vibration (Colthup et al., 1975). The negative bands below  $1050\text{ cm}^{-1}$  likely arise from C-O-S stretching vibrations. Positive bands were assigned to the products of photolysis as follows (Colthup et al., 1975; Barth et al., 1997): the band at  $1688\text{ cm}^{-1}$  to the ketone group of 2-nitrosoacetophenone (4; see Fig. 1), the bands at  $1424$  and  $1378\text{ cm}^{-1}$  to the *cis*-nitroso dimer of the nitrosoketone (4), the small band at  $1269\text{ cm}^{-1}$  to the corresponding *trans*-nitroso dimer, and the intense, broad band at  $1104\text{ cm}^{-1}$  to the released sulfate anion.

For additional confirmation that product (4) in Fig. 1 was the reaction by-product of the caged moiety, photolysis was repeated in the presence of DTT at pH 6 and  $35^\circ\text{C}$  (data not shown). A set of time-resolved spectra had identical transitions to those described previously for the same by-product derived from photolysis of caged ATP and terminated in a spectrum characteristic of 3-methylantranil (Barth et al., 1997). Bands at  $1644$  and  $1466\text{ cm}^{-1}$  in  $^2\text{H}_2\text{O}$  are particularly relevant to the latter assignment. The agreement of the caged sulfate spectra with the caged ATP spectra in the presence and absence of DTT suggests that the photolysis mechanism of caged sulfate is the same as that of caged ATP and that the expected nitrosoketone and sulfate products are formed. The photolysis reaction is as shown in Fig. 1, where  $\text{OR} = \text{OSO}_3^-$  for caged sulfate.

The quantum yield for photolysis of caged sulfate, measured relative to that for 1-(2-nitrophenyl)ethyl phosphate ( $Q_p = 0.54$  (Kaplan et al., 1978)) was 0.47. The *aci*-nitro decay rate constant at pH 7.0 was  $34\text{ s}^{-1}$  and  $250\text{ s}^{-1}$  at pH 6.0 (both measurements at  $20^\circ\text{C}$ ). These values are for data in a well-buffered solution, and in general for caged compounds the *aci*-nitro decay is the rate-determining step for release of final products. In fact this has been rigorously shown in only a few cases, but it was confirmed here by measuring the integrated areas under the bands at 1461, 1331, and  $1101\text{ cm}^{-1}$  with respect to time after the flash for a time series of spectra corresponding to the conditions of Fig. 3 A. As discussed above, the first two of these bands are characteristic of the *aci*-nitro intermediate whereas the large  $1101\text{-cm}^{-1}$  band is from the released sulfate. At pH 8.5 and  $1^\circ\text{C}$ , the average rate constant determined for decay of the two *aci*-nitro bands was  $0.78\text{ s}^{-1}$ , and the rate for formation of the sulfate band was  $0.80\text{ s}^{-1}$ . Proton release is very much faster (see above), and in many applications of the reagent as a caged proton, the rapid acidification of solutions would also accelerate sulfate release. The photolysis efficiency of caged sulfate in the FTIR spectrometer was

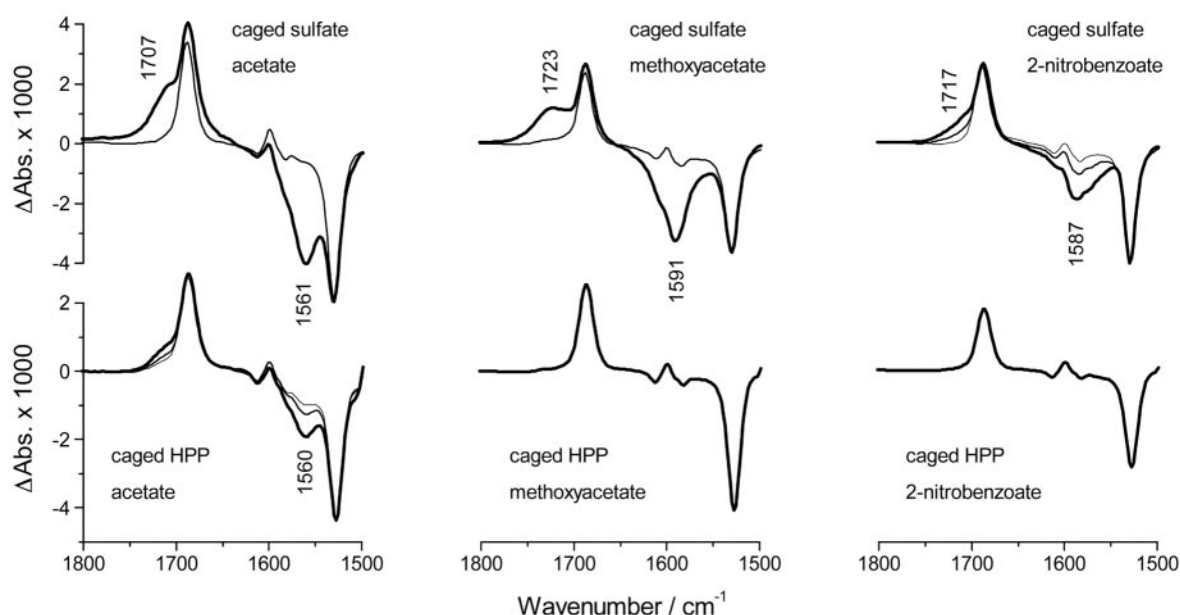


FIGURE 4 Comparison of the protonation abilities of caged sulfate and caged HPP in  $^2\text{H}_2\text{O}$ . The samples contained carboxylate compounds of decreasing pK from left to right (acetate, pK 4.75; methoxyacetate, pK 3.57; 2-nitrobenzoate, pK 2.21). The top panels show a part of the difference spectra for photolysis of caged sulfate, and the lower panels show corresponding spectra for photolysis of caged HPP. Spectra of up to three consecutive flashes on one sample are shown, and the thickness of the line decreases with increasing flash number. Spectra of the second and third flashes are normalized to an identical amplitude of the negative band at  $1527\text{ cm}^{-1}$  for a better comparison.

26%, similar to a value of 28% measured for caged ATP at the same time.

### pH jumps generated with caged sulfate

Photolysis of caged sulfate releases  $\text{SO}_4^{2-}$ , for which the pK of protonation to  $\text{HSO}_4^-$  is 1.92. Therefore, any group with  $\text{pK} > 2$  should be protonated upon photolysis of this reagent. This expectation was tested with a series of carboxylate compounds, which are used here as IR pH indicators because their protonation can easily be monitored. The carboxylate compounds used were acetate (pK 4.75), methoxyacetate (pK 3.57), 2-nitrobenzoate (pK 2.21), and trifluoroacetate (pK 0.52). All pK values refer to dilute aqueous solutions at  $25^\circ\text{C}$  (Sergeant and Dempsey, 1979).

Fig. 3 B compares the IR difference spectra of caged sulfate photolysis obtained with (*thin lines*) and without (*bold lines*) acetate in  $^1\text{H}_2\text{O}$ , in both cases without additional buffer salts. Note that these spectra and those in Fig. 4 contain no time-resolved information as they aim only to probe the capacity of the caged sulfate reagent to protonate carboxylates of different pK values. The spectra with and without acetate are similar with the exception of signals characteristic for carboxylate protonation, i.e., two negative bands near  $1412$  and  $1555\text{ cm}^{-1}$  for the carboxylate ion (symmetric and antisymmetric stretching vibration, respectively) and a positive band near  $1711\text{ cm}^{-1}$  from the  $\text{C}=\text{O}$  group of the carboxylic acid. The differences between the

spectra in the presence and absence of acetate demonstrate that caged sulfate protonates acetate upon photolysis.

The carboxylate protonation signals are more intense in  $^2\text{H}_2\text{O}$  (Fig. 3 C). This is particularly so for the negative band of the antisymmetric stretching vibration at  $1561\text{ cm}^{-1}$  whose extinction coefficient is larger in  $^2\text{H}_2\text{O}$  than in  $^1\text{H}_2\text{O}$  (Chirgadze et al., 1975; Venyaminov and Kalnin, 1990). Thus, only spectra in  $^2\text{H}_2\text{O}$  are shown for the other carboxylates. Experiments were also performed in  $^1\text{H}_2\text{O}$  because the quoted pK values refer to  $^1\text{H}_2\text{O}$  and are usually different from those in  $^2\text{H}_2\text{O}$  (Schowen and Schowen, 1982). However, we did not detect significant differences between the protonation capacity of caged sulfate in  $^1\text{H}_2\text{O}$  and  $^2\text{H}_2\text{O}$ .

The upper panels of Fig. 4 show spectra of carboxylate protonation caused by photolysis of caged sulfate in the spectral range that includes the antisymmetric stretching vibration of  $\text{COO}^-$  and the  $\text{C}=\text{O}$  stretching vibration of  $\text{COOH}$ . The top left panel indicates that 10 mM acetate is completely protonated upon photolysis of  $\sim 26$  mM caged sulfate: the first flash (*bold line*) generates the protonation signals at  $1561$  and  $1707\text{ cm}^{-1}$ , and no further protonation is observed in the second flash (*thin line*). The same is observed for methoxyacetate in the top middle panel. Protonation is even observed for 2-nitrobenzoate but is not complete in the first flash; the second flash causes additional protonation, indicating that more caged sulfate has to be photolyzed for full protonation. This is largely because

the pK of 2-nitrobenzoate is close to that of sulfate, so the two anions compete for the released protons. As expected, no protonation is observed for trifluoroacetate, which is a weaker base than sulfate, and the difference spectrum for photolysis in the presence of trifluoroacetate was nearly identical to that measured without added carboxylate compounds (data not shown). We note, however, that even without the buffering effect of the released sulfate ion, maximal proton release from complete photolysis of 100 mM caged sulfate would reach only pH 1 and therefore could not cause significant protonation of trifluoroacetate. The same qualitative results for each carboxylate were obtained in  $^1\text{H}_2\text{O}$ , demonstrating that the photolysis of caged sulfate protonates groups with pK values down to  $\sim 2.2$ . Caged sulfate can therefore be used to generate large acidification steps.

The experimental conditions here are close to those of other IR studies of protein reactions (reviewed in Zscherp and Barth, 2001) that often use protein concentrations close to 1 mM. If the protein contains, for example, 10 protonatable residues with pK values down to 3.5, the above experiments demonstrate that complete protonation would be achieved by photolysis of  $\sim 26$  mM caged sulfate.

### Comparison with other caged protons

The pH jumps achieved with caged sulfate are larger than those obtained with caged HPP, as demonstrated by repeating the above series of experiments with caged HPP. Results are given in the lower panels of Fig. 4, which show that protonation is only observed for acetate (*lower left panel*) but to a lesser extent than with caged sulfate. This is in line with the pK of the 2-hydroxyphenyl phosphate released on photolysis of caged HPP (see above), which results in buffering of the released proton. The 2-nitrobenzaldehyde compounds (6) and (7) described above were not investigated in this study, because their photolysis produces a carboxylate group from an aldehyde, giving rise to large IR signals that would overlap with those for the protonation of carboxylate groups. In consequence it would be difficult with these compounds to follow the protonation of protein carboxylate groups that are the dominant buffering protein groups near pH 4.

### Titration of Mb with caged sulfate

To demonstrate the biological applicability of caged sulfate for pH jump experiments, we used the well characterized acid-induced conformational change of Mb near pH 4 from its native state to a partially unfolded form (Sage et al., 1991; Chi and Asher, 1998; Palaniappan and Bocian, 1994) that involves opening of the heme pocket and protonation of His93. This breaks the bond between His93 and the heme iron, causing a change in coordination of the iron with

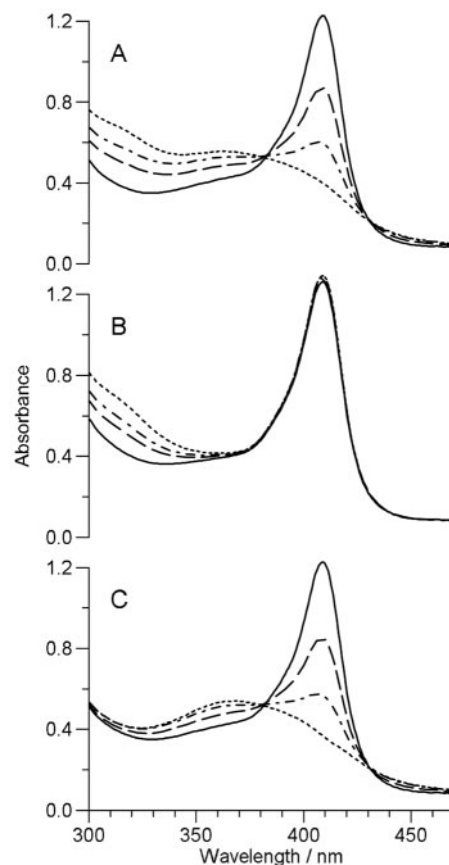


FIGURE 5 UV-visible spectra of the partial unfolding transition of Mb induced by photolysis of caged sulfate: —, spectrum before the first photolysis flash; - - -, spectrum after one flash; - · -, spectrum after two flashes; · · ·, spectrum after five flashes. (A) Raw titration spectra obtained with an unbuffered solution of Mb; (B) Control spectra obtained in 50 mM sodium acetate, pH 4.6; (C) Corrected titration spectra where the absorbance change of caged sulfate has been subtracted (see Materials and Methods). Conditions for all experiments were as follows: initial pH 4.6, 0.11 mM Mb, and 2.5 mM caged sulfate.

consequent broadening of the Soret band and a shift of its maximum from 409 to 363 nm. We reproduced these results in a titration of a solution of Mb in 100 mM NaCl with hydrochloric acid in a 1-cm cuvette. In our hands the transition started at pH 4.6 and was 90% complete at pH 4.2, with a midpoint at pH 4.4 (data not shown), in very good agreement with  $\text{pK}_{\text{eff}} 4.33$  as determined by Sage et al. (1991) in 100 mM phosphate buffer. This titration served to correlate pH values with Mb spectra in the photolytic acidifications (see below).

The titration was repeated by flash photolysis of a solution of 2.5 mM caged sulfate and 0.11 mM Mb in 100 mM NaCl. The raw titration spectra are shown in Fig. 5 A. The solid line shows the spectrum before photolysis of caged sulfate, where the Soret band is maximal at 409 nm. With subsequent flashes, this band is reduced and the absorbance increases below 380 nm. The latter change arises from a

combination of the shift of the Soret band to lower wavelength and changes in the spectrum of the caged sulfate upon photolysis. The absorbance changes arising from photolysis of the caged sulfate are observed for all nitrobenzyl- and nitrophenylethyl-caged compounds (see Fig. 1 *a* of Peng and Goeldner, 1996, for a typical example). To separate these contributions, a control sample buffered at pH 4.6 with sodium acetate was investigated. The control spectra in Fig. 5 *B* show minimal changes to the Soret band upon successive flash irradiation of this sample, demonstrating that suppression of the pH jump allows Mb to remain in its native form. However, the control spectra do show the changes below 370 nm that arise from the photolysis of caged sulfate alone. These absorbance changes were subtracted from the raw titration spectra (see Materials and Methods), and the corrected titration spectra are shown in Fig. 5 *C*. Without the perturbation by the absorbance changes of caged sulfate, they clearly show the shifted Soret band with its maximum near 365 nm.

In a second control experiment, spectra of solutions of 0.11 mM Mb in 100 mM NaCl with additions of 20 mM hydrochloric acid were recorded in the microcuvette under conditions close to those of the photochemically induced titration described above. An increment of  $\sim 2$  mM in the added proton concentration was required to induce the full conformational transition of Mb. This agrees well with the result that 2.5 mM caged sulfate had to be photolyzed almost to completion to obtain the same transition.

By comparison of the spectra from the caged sulfate photochemical titration and the hydrochloric acid titration in the 1-cm-path-length cuvette, the pH in the Mb/caged sulfate samples after two flashes was deduced to be  $\sim 4.3$ , after three flashes  $\sim 4.1$ , and after five flashes  $< 3.9$ . This showed that caged sulfate had generated a pH jump well below pH 4.0, thereby inducing the partial unfolding transition of Mb, and thus can be used for protein folding studies in that pH range.

The results described above establish the potential of caged sulfate as a new caged proton that is capable of effecting sub-microsecond acidification steps of sufficient amplitude to effect protonation of most carboxylate groups of biological relevance. This highly water-soluble and thermally stable compound has the ability to effect the largest pH jumps of any caged proton reagent currently available. Furthermore, the absence of carboxylate groups in the reagent or its photoproducts makes it suitable to observe protonation changes of carboxylates with IR spectroscopy. Applications of the reagent will be described elsewhere.

We are grateful to Professor W. Mäntele for his continuous support, to Dr. D. R. Trentham for measurement of the *aci*-nitro decay kinetics, and to Dr. V. R. N. Munasinghe for technical assistance with preparation of caged sulfate. We thank the MRC Biomedical NMR Center for access to facilities.

This work was funded in part by a Royal Society European Science Exchange Program grant.

## REFERENCES

- Abbruzzetti, S., C. Viappiani, J. R. Small, L. J. Libertini, and E. W. Small. 2000. Kinetics of local helix formation in poly-L-glutamic acid studied by time-resolved photoacoustics: neutralization reactions of carboxylates in aqueous solutions and their relevance to the problem of protein folding. *Biophys. J.* 79:2714–2721.
- Adams, S. R., and R. Y. Tsien. 1993. Controlling cell chemistry with caged compounds. *Annu. Rev. Physiol.* 55:755–784.
- Barth, A. 1999. Phosphoenzyme conversion of the sarcoplasmic reticulum  $\text{Ca}^{2+}$  ATPase: molecular interpretation of infrared difference spectra. *J. Biol. Chem.* 274:22170–22175.
- Barth, A., J. E. T. Corrie, M. J. Gradwell, Y. Maeda, W. Mäntele, T. Meier, and D. R. Trentham. 1997. Time-resolved infrared spectroscopy of intermediates and products from photolysis of 1-(2-nitrophenyl)ethyl phosphates: reaction of the 2-nitrosoacetophenone byproduct with thiols. *J. Am. Chem. Soc.* 119:4149–4159.
- Barth, A., K. Hauser, W. Mäntele, J. E. T. Corrie, and D. R. Trentham. 1995. Photochemical release of ATP from 'caged ATP' studied by time-resolved infrared spectroscopy. *J. Am. Chem. Soc.* 117:10311–10316.
- Barth, A., W. Mäntele, and W. Kreutz. 1990. Molecular changes in the sarcoplasmic reticulum  $\text{Ca}^{2+}$  ATPase during catalytic activity: a Fourier transform infrared (FTIR) study using photolysis of caged ATP to trigger the reaction cycle. *FEBS Lett.* 277:147–150.
- Barth, A., F. von Germar, W. Kreutz, and W. Mäntele. 1996. Time-resolved infrared spectroscopy of the  $\text{Ca}^{2+}$  ATPase: the enzyme at work. *J. Biol. Chem.* 271:30637–30646.
- Barth, A., and C. Zscherp. 2000. Substrate binding and enzyme function investigated by infrared spectroscopy. *FEBS Lett.* 477:151–156.
- Bonetti, G., A. Veccli, and C. Viappiani. 1997. Reaction volume of water formation detected by time-resolved photoacoustics: photoinduced proton transfer between *o*-nitrobenzaldehyde and hydroxyls in water. *Chem. Phys. Lett.* 269:268–273.
- Cheng, H., S. Sukal, H. Deng, T. S. Leyh, and R. Callender. 2001. Vibrational structure of GDP and GTP bound to ras: an isotope-edited FTIR study. *Biochemistry.* 40:4035–4043.
- Chi, Z., and S. A. Asher. 1998. UV resonance Raman determination of protein acid denaturation: selective unfolding of helical segments of horse myoglobin. *Biochemistry.* 37:2865–2872.
- Chirgadze, Y. N., O. V. Fedorov, and N. P. Trushina. 1975. Estimation of amino acid residue side chain absorption in the infrared spectra of protein solutions in heavy water. *Biopolymers.* 14:679–694.
- Colthup, N. B., L. H. Daly, and S. E. Wiberley. 1975. Introduction to Infrared and Raman Spectroscopy, 2nd ed. Academic Press, New York.
- Corrie, J. E. T., B. C. Gilbert, V. R. N. Munasinghe, and A. C. Whitwood. 2000. EPR studies of the structure of transient radicals formed in photolytic reactions of some 2-nitrobenzyl compounds: characterisation of aryl alkoxy aminoxyls and nitroaromatic radical-anions in the photolysis of caged ATP and related compounds. *J. Chem. Soc. Perkin Trans. 2* 2483–2491.
- Corrie, J. E. T., G. P. Reid, D. R. Trentham, M. B. Hursthouse, and M. A. Mazid. 1992. Synthesis and absolute stereochemistry of the 2 diastereoisomers of  $P^3$ -1-(2-nitrophenyl)ethyl adenosine-triphosphate (caged ATP). *J. Chem. Soc. Perkin Trans. 1* 1015–1019.
- Corrie, J. E. T., and D. R. Trentham. 1993. Caged nucleotides and neurotransmitters. In *Bioorganic Photochemistry*. H. Morrison, editor. Wiley, New York. 243–305.
- Il'ichev, Y. V., and J. Wirz. 2000. Rearrangements of 2-nitrobenzyl compounds. I. Potential energy surface of 2-nitrotoluene and its isomers explored with ab initio and density functional theory methods. *J. Phys. Chem. A.* 104:7856–7870.
- Gutman, M., D. Huppert, and E. Pines. 1981. The pH jump: a rapid modulation of pH of aqueous solutions by a laser pulse. *J. Am. Chem. Soc.* 103:3709–3713.
- Janko, K., and J. Reichert. 1987. Proton concentration jumps and generation of transmembrane pH-gradients by photolysis of 4-formyl-6-methoxy-3-nitrophenoxycetic acid. *Biochim. Biophys. Acta.* 905:409–416.

- Jayaraman, V., S. Thiran, and D. R. Madden. 2000. Fourier transform infrared spectroscopic characterization of a photolabile precursor of glutamate. *FEBS Lett.* 475:278–282.
- Kaplan, J. H. 1990. Photochemical manipulation of divalent-cation levels. *Annu. Rev. Physiol.* 52:897–914.
- Kaplan, J. H., B. Forbush, and J. F. Hoffman. 1978. Rapid photolytic release of ATP from a protected analogue: utilization by the Na:K pump of human red blood cell ghosts. *Biochemistry.* 17:1929–1935.
- Khan, S., F. Castellano, J. L. Spudich, J. A. McCray, R. S. Goody, G. P. Reid, and D. R. Trentham. 1993. Excitatory signaling in bacteria probed by caged chemoeffectors. *Biophys. J.* 65:2368–2382.
- McCray, J. A., and D. R. Trentham. 1989. Properties and uses of photo-reactive caged compounds. *Annu. Rev. Biophys. Biophys. Chem.* 18: 239–270.
- Marriott, G., editor. 1998. Caged Compounds: Methods in Enzymology, Vol. 291. Academic Press, San Diego.
- Palaniappan, V., and D. F. Bocian. 1994. Acid-induced transformations of myoglobin: characterization of a new equilibrium heme-pocket intermediate. *Biochemistry.* 33:14264–14274.
- Peng, L., and M. Goeldner. 1996. Synthesis and characterization of photolabile choline precursors as reversible inhibitors of cholinesterases: release of choline in the microsecond time range. *J. Org. Chem.* 61: 185–191.
- Perrin, D. D. 1982. Ionisation Constants of Inorganic Acids and Bases in Aqueous Solution, 2nd ed. Pergamon, Oxford.
- Sage, J. T., D. Morikis, and P. M. Champion. 1991. Spectroscopic studies of myoglobin at low pH: heme structure and ligation. *Biochemistry.* 30:1227–1237.
- Schowen, K. B., and R. L. Schowen. 1982. Solvent isotope effects on enzyme-systems. *Methods Enzymol.* 87:551–606.
- Schwörer, M., and J. Wirz. 2001. Photochemical reaction mechanisms of 2-nitrobenzyl compounds in solution. I. 2-Nitrotoluene: thermodynamic and kinetic parameters of the *aci*-nitro tautomer. *Helv. Chim. Acta.* 84:1441–1457.
- Sergeant, E. P., and B. Dempsey. 1979. Ionisation Constants of Organic Acids in Aqueous Solution. Pergamon, Oxford.
- Tserng, K. Y., and P. D. Klein. 1977. Synthesis of sulfate esters of lithocholic acid, glycolithocholic acid and tauroolithocholic acid with sulfur trioxide–triethylamine. *J. Lipid Res.* 18: 491–495.
- Venyaminov, S. Y., and N. N. Kalnin. 1990. Quantitative IR spectrophotometry of peptide compounds in water (H<sub>2</sub>O) solutions. I. Spectral parameters of amino acid residue absorption bands. *Biopolymers.* 30: 1243–1257.
- Walker, J. W., G. P. Reid, J. A. McCray, and D. R. Trentham. 1988. Photolabile 1-(2-nitrophenyl)ethyl phosphate esters of adenine nucleotide analogs: synthesis and mechanism of photolysis. *J. Am. Chem. Soc.* 110:7170–7177.
- Wettermark, G., E. D. Black, and L. Dogliotti. 1965. Reactions of photochemically formed transients from 2-nitrotoluene. *Photochem. Photobiol.* 4:229–239.
- Zscherp, C., and A. Barth. 2001. Reaction-induced infrared difference spectroscopy for the study of protein reaction mechanisms. *Biochemistry.* 40:1875–1883.